

Temephos spraying and thermal fogging efficacy on *Aedes aegypti* in homogeneous urban residences

Karunia Putra Wijaya^{a,*}, Thomas Goetz^b, Edy Soewono^a, Nuning Nuraini^a

^a Department of Mathematics, Bandung Institute of Technology, Bandung 40132, Indonesia

^b Mathematical Institute, University of Koblenz, 56070 Koblenz, Germany

*Corresponding author, e-mail: karuniaputra@s.itb.ac.id

Received 7 Jan 2013

Accepted 5 Apr 2013

ABSTRACT: An optimal control model of *Aedes aegypti* population dynamics concerning classification of indoor-outdoor life cycles is taken into account in this paper. A dengue epidemics measure, the basic mosquito offspring, is obtained from the well-known next-generation matrix. The number is used to analyse the stability of the mosquito-free equilibrium. This mosquito-free equilibrium describes a steady-state condition in the mosquito population dynamics where there are no mosquitoes. Comprehensive analysis on the existence and stability of the positive non-trivial equilibrium state is shown as well. Further work deals with designation of the control measures and numerical implementation of the optimal control model using various scenarios. We highlight those measures expressed as the semi-discrete mass profile of the Temephos spraying and the thermal fogging.

KEYWORDS: indoor-outdoor life cycles, the basic mosquito offspring, the mosquito-free equilibrium, optimal control

INTRODUCTION

In recent decades, the impacts of dengue flavivirus on humans have become a global health concern. They range from asymptomatic infections to symptoms incorporated with severe circulatory shocks and haemorrhagic vascular leaks. The World Health Organization has published guidelines for clinical management including diagnostic methods in dengue surveillance and vector controls. Controlling dengue vector has been perceived to be more effective than curing flavivirus transmission in human blood. The four flavivirus serotypes (DEN 1-4) are primarily transmitted by infected female *A. aegypti*^{1,2}. People worldwide have investigated the temporal and spatial dynamics of *A. aegypti* population by means of endogenous forces and climate change^{3,4}. This species has been crowned as the main transmitter of dengue diseases in tropical countries, although typical diseases have successfully been transmitted by *A. albopictus* in some areas in Asia⁵. A particular dengue disease is endemic in several countries worldwide and public costs to pay the lethal effects caused by the disease have been risen significantly. Dengue diseases have threatened about 2.5 billion people per year. However, there are no licensed vaccines or antivirals for preventing the transmission of all flavivirus serotypes in human blood^{6,7}. Vector control will one day be used as an additional key determinant in suppressing the dengue

persistence around the world.

The main vector control proposed in this paper consists of two schematic processes. First, suppression of the size of indoor immature phases by using Temephos spraying. The Temephos spraying is mainly used to kill mosquito larvae rather than to kill eggs and pupae^{8,9}. Second, suppression of the size of indoor-outdoor mature phases by using thermal fogging. The thermal fogging is composed of chemicals used to disrupt respiration of larvae, pupae, and adults.

A. aegypti mosquitoes lay their eggs on calm and clean water environment. They lay their eggs in three to five batches during their lifetime, resulting approximately 100–200 units in each laying time¹⁰. In terms of quantity, the size of available blood meal determines the number of produced eggs in the field¹¹. It is known that *Aedes* larvae (respectively pupae) can live in water for 5–10 days (7–13 days)¹². The length of the larval-period depends on water temperature and air humidity. A group of larvae particularly grows in an existing site with restricted logistic availability. In order to maintain its life within this restriction, a larva competes with its own¹³. Moreover, it is known that both male and female *A. aegypti* adults can survive for 0.7 days (female) and 5.8 days (male) on average¹⁴.

Based on the nature of breeding site, the origin of the first three phases of *A. aegypti* proliferation are classified into two major locations: indoor and

outdoor. In urban areas, mosquito newborns from outdoor contribute significantly to the rise of the entire *A. aegypti* population size. The size of mosquito population increases as the number of proper sites increases after rainfall.

In this study, we construct an optimal control scheme as a strategy in determining the decision-making process. The result will determine expenses related to accumulated daily costs of *A. aegypti* control. The optimal control model construction is motivated by Caetano et al¹⁵, which was currently focused on using the continuous-time control. We highlight the other motivational paper on mosquito reduction, where the author gives a prime importance to the use of the sterile insect technique¹⁶. Due to an appearance of need of precise daily treatment, construction of an optimal control model regulated by a unified daily-valued control is needed. The daily-valued control (semi-discrete control) seems accurate in claiming how many daily dosages of chemicals we need to suppress the size of *A. aegypti* population.

MOSQUITO POPULATION DYNAMICS MODEL

We construct the mosquito population dynamics model involving the presence of control. Mathematically, the entire *A. aegypti* population is divided into five time-dependent compartments: the indoor egg $E_1(t)$, the outdoor egg $E_2(t)$, the indoor larva $L_1(t)$, the outdoor larva $L_2(t)$, and the adult $A(t)$. The presence of pupa is ignored in the model since it has similar adaptation characteristics and life duration compared to larva. The mosquito population is assumed to be homogeneous, meaning that every single individual in a particular compartment can homogeneously be mixed with its own. All mosquitoes are considered to live too concisely to develop resistance against the two proposed chemicals.

Two time-dependent control measures are added to the model to suppress the size of the mosquito population, represented by the Temephos spraying and the thermal fogging. The corresponding masses are denoted by $u_1(t)$ (for the Temephos spraying) and $u_2(t)$ (for the thermal fogging) with the unit of mg. We introduce the dimension modifier constants $w_i, i = 1, 2$ (1/mg×1/day). Each constant converts 1 mg of an associated control measure to the negative growth rate of treated compartments. The Temephos spraying basically kills a group of larvae before they turn into pupae and also makes the eggs impotent. The thermal fogging basically kills a group of mosquito adults, but it also blocks the underwater respiration process of larvae. The effectivity of the Temephos

spraying on the size of the indoor egg and the effectivity of the thermal fogging on the size of the indoor and outdoor larva is described by the constants q_1, q_2 , and q_3 , respectively.

The observed area is assumed to be near homogeneous water containers, both indoor and outdoor. Depending on the size of the area, it is supposed that the ratio of the size of the outdoor to the size of the indoor water containers is represented by m . Realistically, we assume $m > 1$. Here we want to estimate the average size of both immature and mature phases of *A. aegypti* in and nearby each house.

It is assumed that the adult will choose an indoor breeding site with the preference probability p equipped by the adult-derived birth rate ϕ (1/day). The natural mortality rates for each compartment are denoted by $\mu_i, i = 1, \dots, 5$ (1/day). The age-transitional rates are denoted by $\alpha_i, i = 1, \dots, 4$ (1/day). The logistic coefficients $\sigma_i, i = 1, 2$ (1/individual×1/day) take into account the carrying capacities of the water container for the larva, both indoor and outdoor. In our model, we use the estimate $\sigma_2 \approx \sigma_1/m$.

Let $x(t) = [E_1(t), E_2(t), L_1(t), L_2(t), A(t)]$ are referred to as the state variables and $u(t) = [u_1(t), u_2(t)]$ are referred to as the control variables. Including the time-dependence, we have $x : [0, T] \rightarrow \mathbb{R}^5$ and $u : [0, T] \rightarrow \mathbb{R}^2$. Our *A. aegypti* population dynamics model is given by the system

$$\dot{x}(t) = F(x(t), u(t)), F : \mathbb{R}^5 \times \mathbb{R} \rightarrow \mathbb{R}^5, \quad (1)$$

written component-wise as

$$\begin{aligned} \dot{E}_1(t) &= p\phi A(t) - \alpha_1 E_1(t) \\ &\quad - q_1 w_1 u_1(t) E_1(t) - \mu_1 E_1(t) \end{aligned} \quad (2a)$$

$$\begin{aligned} \dot{E}_2(t) &= (1-p)\phi A(t) - \alpha_2 E_2(t) \\ &\quad - \mu_2 E_2(t) \end{aligned} \quad (2b)$$

$$\begin{aligned} \dot{L}_1(t) &= \alpha_1 E_1(t) - \sigma_1 L_1(t)^2 - \alpha_3 L_1(t) \\ &\quad - w_1 u_1(t) L_1(t) - q_2 w_2 u_2(t) L_1(t) \\ &\quad - \mu_3 L_1(t) \end{aligned} \quad (2c)$$

$$\begin{aligned} \dot{L}_2(t) &= \alpha_2 E_2(t) - \sigma_2 L_2(t)^2 - \alpha_4 L_2(t) \\ &\quad - q_3 w_2 u_2(t) L_2(t) - \mu_4 L_2(t) \end{aligned} \quad (2d)$$

$$\begin{aligned} \dot{A}(t) &= \alpha_3 L_1(t) + \alpha_4 L_2(t) - w_2 u_2(t) A(t) \\ &\quad - \mu_5 A(t). \end{aligned} \quad (2e)$$

The system (1) is supplemented by the positive initial condition $x_0 \in \mathbb{R}^5$.

Our current objectives are suppressing the size of each compartment and minimizing the cost for control implementation. It is observed from the model that somehow we need big values for control measures in

order to significantly suppress the size of particular treated compartments. This will result in a high cost for the control. In this case, we need a certain balance compromising this control-compartments problem. This required balance is expressed as the real-valued objective function

$$J(x, u) = \frac{1}{2T} \int_0^T \sum_{i=1}^5 \omega_{x,i} x_i^2(t) + \sum_{j=1}^2 \omega_{u,j} u_j^2(t) dt. \quad (3)$$

The trade-off coefficients $\omega_{x,i} > 0, i = 1, \dots, 5$ and $\omega_{u,j} > 0, j = 1, 2$ are used to equalize the influence of x_i^2 and u_j^2 in the objective function. As a rule-of-thumb, typical values for these coefficients behave like

$$\frac{\omega_{x,i}}{\omega_{u,j}} \approx \frac{\bar{u}_j^2}{\bar{x}_i^2} \quad (4)$$

where \bar{u}_j is the value of the empirical control measure used to suppress the size of the associated empirical state variable \bar{x}_i in the field. The length of observation time $T > 0$ is assumed to be fixed.

Control design

We assume that both control measures $u_1(t)$ and $u_2(t)$ are piecewise constant and change every h_1 and h_2 days, respectively. Hence we introduce the two ($i = 1, 2$) sets of discrete time-points $t_{i,j} = jh_i$ where $j = 0, \dots, \lceil (T/h_i) \rceil$. We model the control measures as follows

$$u_i(t) = \sum_{0 \leq j \leq \lceil (T/h_i) \rceil} a_{ij} \mathbf{1}_{[t_{i,j}, t_{i,j+1})}(t) \quad (5)$$

for $i = 1, 2$. Here $\mathbf{1}_{[t_{i,j}, t_{i,j+1})}(t)$ denotes the characteristic function of the time interval $[t_{i,j}, t_{i,j+1})$ and a_{ij} denotes the control measure values at those discrete intervals.

MODEL ANALYSIS

Positively invariant

A biologically meaningful solution of the system $\dot{x} = F(x, 0)$ must be non-negative for all time, provided that the given initial value is non-negative. The following theorem states this result.

Theorem 1 *Let x_0 be given positive vector-valued initial value of the uncontrolled system (1), i.e., $\dot{x} = F(x, 0)$. Then the solution x has positive elements for all $t > 0$.*

Proof: The uncontrolled system $\dot{x} = F(x, 0)$ induces a flow in \mathbb{R}^5 . We show, that the domain $\Omega = \mathbb{R}_+^5 = \{x_i \geq 0, i = 1, \dots, 5\}$ is invariant under this flow. Let n_x denote the outer normal at a boundary point $x \in \partial\Omega$. Then an easy calculation shows, that

$$n_x^T F(x, 0) \leq 0$$

for all $x \in \partial\Omega$. Hence, trajectories cannot leave the domain Ω . \square

Equilibria

The system $\dot{x} = F(x, 0)$ possesses trivial and non-trivial equilibria. These equilibrium points can be obtained by solving the five stationary equations (2). After some algebraic manipulations, we arrive at following reduction:

$$L_1^{*2} + \chi_1 L_1^* - \varepsilon_1 \alpha_4 L_2^* = 0, \quad (6a)$$

$$L_2^{*2} + \chi_2 L_2^* - \varepsilon_2 \alpha_3 L_1^* = 0, \quad (6b)$$

where

$$\varepsilon_1 = \frac{\alpha_1 p \phi}{(\alpha_1 + \mu_1) \mu_5 \sigma_1},$$

$$\varepsilon_2 = \frac{\alpha_2 (1-p) \phi}{(\alpha_2 + \mu_2) \mu_5 \sigma_2},$$

$$\chi_1 = \frac{\alpha_3 (1 - \sigma_1 \varepsilon_1) + \mu_3}{\sigma_1},$$

$$\chi_2 = \frac{\alpha_4 (1 - \sigma_2 \varepsilon_2) + \mu_4}{\sigma_2}.$$

Given the positive roots (L_1^*, L_2^*) of (6), we obtain the remaining three components of the positive equilibrium state as a function of $\Lambda = \alpha_3 L_3^* + \alpha_4 L_2^*$:

$$x^* = (E_1^*(\Lambda), E_2^*(\Lambda), L_1^*, L_2^*, A^*(\Lambda)) = \left(\frac{p\phi}{(\alpha_1 + \mu_1) \mu_5} \Lambda, \frac{(1-p)\phi}{(\alpha_2 + \mu_2) \mu_5} \Lambda, L_1^*, L_2^*, \frac{1}{\mu_5} \Lambda \right).$$

The following theorem explains the existence and stability of the positive non-trivial equilibrium state (L_1^*, L_2^*).

Theorem 2 *Let $\varepsilon_1, \varepsilon_2, \chi_1$ and χ_2 be defined as above. In any of*

Case 1 $\chi_1, \chi_2 < 0$;

Case 2 $\chi_1 < 0$ and $\chi_2 > 0$ or $\chi_1 > 0$ and $\chi_2 < 0$ or $\chi_1 \chi_2 = 0$;

Case 3 $\chi_1, \chi_2 > 0$ and $\chi_1 \chi_2 < \varepsilon_1 \varepsilon_2 \alpha_3 \alpha_4$;

there exists a unique positive equilibrium state (L_1^, L_2^*) which is asymptotically stable.*

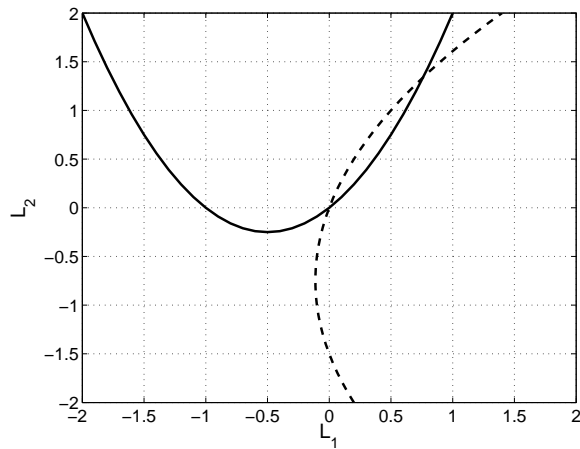


Fig. 1 Schematic view of the two curves $L_2 = f(L_1)$ (solid line) and $L_1 = g(L_2)$ (dashed line) in Case 3.

Proof: First we consider the existence of a unique positive root of the two equations (6). Eq. (6a) gives rise to a curve $L_2 = f(L_1) := (1/\varepsilon_1\alpha_4)L_1(L_1 + \chi_1)$ in the L_1L_2 -plane. Similarly, we can interpret (6b) as a curve $L_1 = g(L_2) := (1/\varepsilon_2\alpha_3)L_2(L_2 + \chi_2)$. By examining the three cases separately, we obtain the existence of a unique intersection point (L_1^*, L_2^*) of the two curves in the first quadrant. For the first two cases this is rather obvious, whereas the third case requires some consideration. In Fig. 1 we depict the situation of Case 3. An intersection of the two curves in the first quadrant only exists, provided the slopes satisfy $f'(0) < 1/g'(0)$, i.e., $\chi_1/\varepsilon_1\alpha_4 < \varepsilon_2\alpha_3/\chi_2$ or $\chi_1\chi_2 < \varepsilon_1\varepsilon_2\alpha_3\alpha_4$.

Note, that in all three cases, the slope of the two curves at the positive equilibrium state (L_1^*, L_2^*) are given by $f'(L_1^*) = (1/\varepsilon_1\alpha_4)(2L_1^* + \chi_1)$ and $g'(L_2^*) = (1/\varepsilon_2\alpha_3)(2L_2^* + \chi_2)$. Both slopes are always positive. Furthermore, it always holds that, $f'(L_1^*) > 1/g'(L_2^*)$, i.e.,

$$\frac{2L_1^* + \chi_1}{\varepsilon_1\alpha_4} > \frac{\varepsilon_2\alpha_3}{2L_2^* + \chi_2}. \tag{7}$$

To determine the stability of the unique positive equilibrium state, we compute the eigenvalues of the reduced Jacobian

$$J_L(L_1^*, L_2^*) = \begin{pmatrix} -2\sigma_1L_1^* - \chi_1\sigma_1 & \sigma_1\varepsilon_1\alpha_4 \\ \sigma_2\varepsilon_2\alpha_3 & -2\sigma_2L_2^* - \chi_2\sigma_2 \end{pmatrix}.$$

According to the Routh-Hurwitz-criterion, the eigenvalues of J_L lie in the negative half-plane, if $\text{tr } J_L < 0$ and $\det J_L > 0$.

For the trace, it holds, that

$$\text{tr } J_L = -[\sigma_1(2L_1^* + \chi_1) + \sigma_2(2L_2^* + \chi_2)] < 0,$$

since $2L_i^* + \chi_i > 0$ for both $i = 1$ and $i = 2$.

For the determinant, it holds that

$$\det J_L = \sigma_1\sigma_2[(2L_1^* + \chi_1)(2L_2^* + \chi_2) - \varepsilon_1\alpha_4\varepsilon_2\alpha_3].$$

From (7) it follows that $\det J_L > 0$. □

The basic offspring

Analysing the sensitivity of the constant control to the system (1), we build a real 5×5 matrix, say G , where entry g_{ij} is the number of individual newborns in compartment i produced by an individual in compartment j within an average life period of compartment j 's individual¹⁷. For example, as a single indoor egg produces α_1 indoor larvae per unit time during its productive period $1/(\alpha_1 + q_1w_1u_1 + \mu_1)$, we obtain the according entry $g_{31} = \alpha_1/(\alpha_1 + q_1w_1u_1 + \mu_1)$. The mosquito-free equilibrium ξ is defined as a state, where no agent giving birth to new eggs, larvae, and adults. In this model, the mosquito-free equilibrium equals to the trivial equilibrium. The matrix G evaluated on the mosquito-free equilibrium, i.e., $G|_{x=\xi} = \bar{G}$, will look like

$$\bar{G} = \begin{pmatrix} 0 & 0 & 0 & 0 & k_1 \\ 0 & 0 & 0 & 0 & k_2 \\ k_3 & 0 & 0 & 0 & 0 \\ 0 & k_4 & 0 & 0 & 0 \\ 0 & 0 & k_5 & k_6 & 0 \end{pmatrix}$$

where

$$\begin{aligned} k_1 &= \frac{p\phi}{w_2u_2 + \mu_5}, \\ k_2 &= \frac{(1-p)\phi}{w_2u_2 + \mu_5}, \\ k_3 &= \frac{\alpha_1}{\alpha_1 + q_1w_1u_1 + \mu_1}, \\ k_4 &= \frac{\alpha_2}{\alpha_2 + \mu_2}, \\ k_5 &= \frac{\alpha_3}{\alpha_3 + q_2w_2u_2 + w_1u_1 + \mu_3}, \\ k_6 &= \frac{\alpha_4}{\alpha_4 + q_3w_2u_2 + \mu_4}. \end{aligned}$$

Let $\sigma(\bar{G})$ denotes the spectrum of \bar{G} and let

$$\rho(\bar{G}) = \max_{\lambda \in \sigma(\bar{G})} |\lambda|$$

be the spectral radius of \bar{G} . After some computations we obtain

$$\rho(\bar{G}) = \left| \left(\frac{S}{R} \right)^{1/3} \right|$$

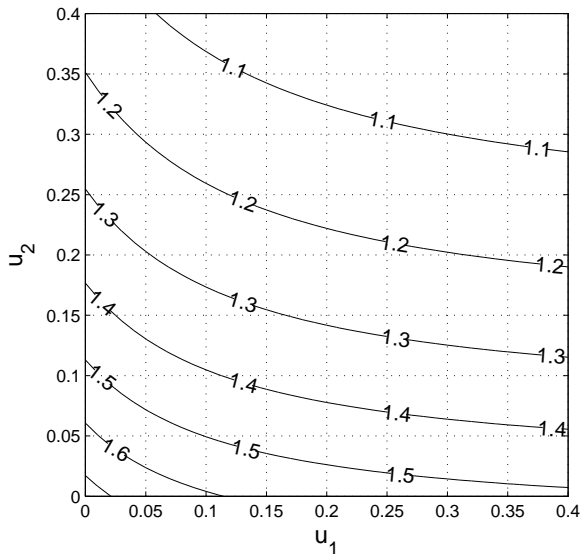


Fig. 2 $\rho(\bar{G})$ with respect to the constant control.

where S and R are algebraic functions of the parameters.

The spectral radius determines whether any population diverges from or converges to the mosquito-free equilibrium on an infinite time horizon. If the population converges for an arbitrary initial value to the mosquito-free equilibrium, we call the mosquito-free equilibrium asymptotically stable. As the matrix \bar{G} becomes a ‘ratio’ between an initial population and a resulting step-forward population, it is concluded that the mosquito-free equilibrium will be stable if $\rho(\bar{G}) < 1$ and is unstable if $\rho(\bar{G}) > 1$. Here we show the contour lines of $\rho(\bar{G})$ with respect to the constant control measures in the domain $[0, 0.4]^2$ while all parameters are defined as in the next section (Fig. 2). \bar{G} and $\rho(\bar{G})$ are well-known as the next generation matrix and the basic mosquito offspring based on the system (1).

OPTIMAL CONTROL PROBLEM

In the sequel we derive optimal control scheme where the optimization problem is written as follows

$$\min_{u \in \mathcal{U}_{ad}} J(x, u) \text{ s.t. } P(x, u) = 0. \tag{8}$$

In this case, $P(x, u) = 0$ is short-hand notation for (1). By $\mathcal{U}_{ad} \subset L^2([0, T]; \mathbb{R}^2)$ we denote the set of admissible controls which is assumed to be compact. To solve the constrained optimization problem (8), we introduce the Lagrangian $\mathcal{L} = X \times Z \times \mathcal{U}_{ad} \rightarrow \mathbb{R}$ defined by

$$\mathcal{L}(x, z, u) = J(x, u) - \langle P(x, u), z \rangle \tag{9}$$

where $X, Z \in L^2([0, T]; \mathbb{R}^5)$ are the two dual spaces for the state and the adjoint variables, respectively. For the according duality product we use the notation $\langle \cdot, \cdot \rangle : X \times Z \rightarrow \mathbb{R}$.

Considering the first-order optimality condition, we need the Lagrangian function \mathcal{L} to satisfy $\nabla \mathcal{L} = 0$ with respect to its three arguments. Zeroing the partial derivative of \mathcal{L} with respect to z , we regain the state (1). Zeroing the partial derivative of \mathcal{L} with respect to x , we gain the adjoint equation completed by the transversality condition (see Ref. 18)

$$\begin{aligned} \dot{z}_i &= -\omega_{x,i}x_i - \nabla_{x_i}F \cdot z, \\ z_i(T) &= 0, \quad i = 1, \dots, 5. \end{aligned} \tag{10}$$

The adjoint equation can be written component-wise as

$$\begin{aligned} \dot{z}_1(t) &= -\omega_{x,1}E_1(t) + [\alpha_1 + q_1w_1u_1(t) \\ &\quad + \mu_1]z_1(t) - \alpha_1z_3(t) \end{aligned} \tag{11a}$$

$$\begin{aligned} \dot{z}_2(t) &= -\omega_{x,2}E_2(t) + (\alpha_2 + \mu_2)z_2(t) \\ &\quad - \alpha_2z_4(t) \end{aligned} \tag{11b}$$

$$\begin{aligned} \dot{z}_3(t) &= -\omega_{x,3}L_1(t) + [2\sigma_1L_1(t) + \alpha_3 \\ &\quad + w_1u_1(t) + q_2w_2u_2(t) \\ &\quad + \mu_3]z_3(t) - \alpha_3z_5(t) \end{aligned} \tag{11c}$$

$$\begin{aligned} \dot{z}_4(t) &= -\omega_{x,4}L_2(t) + [2\sigma_2L_2(t) + \alpha_4 \\ &\quad + q_3w_2u_2(t) + \mu_4]z_4(t) \\ &\quad - \alpha_4z_5(t) \end{aligned} \tag{11d}$$

$$\begin{aligned} \dot{z}_5(t) &= -\omega_{x,5}A(t) \\ &\quad + (w_2u_2(t) + \mu_5)z_5(t) \\ &\quad - p\phi z_1(t) - (1-p)\phi z_2(t). \end{aligned} \tag{11e}$$

Finally, zeroing the partial derivative of \mathcal{L} with respect to u , we find the gradient equation

$$\nabla_u J(x, u) - \langle \nabla_u P(x, u), z \rangle = 0. \tag{12}$$

From this equation, we gain the optimal control

$$u_1^*(t) = - \frac{q_1w_1E_1(t)z_1(t) + w_1L_1(t)z_3(t)}{\omega_{u,1}} \tag{13a}$$

$$\begin{aligned} u_2^*(t) &= - \frac{q_2w_2L_1(t)z_3(t) + q_3w_2L_2(t)z_4(t)}{\omega_{u,2}} \\ &\quad - \frac{w_2A(t)z_5(t)}{\omega_{u,2}}. \end{aligned} \tag{13b}$$

To provide limitation for each control measure, i.e., $u_i(t) \in [a_i, b_i], i = 1, 2$ for all t in $[0, T]$, we use the saturation

$$u_i(t) \mapsto u_i(t) = \begin{cases} a_i, & u_i(t) \leq a_i, \\ b_i, & u_i(t) \geq b_i, \\ u_i(t), & \text{otherwise.} \end{cases} \tag{14}$$

In the optimization project, we use an iterative method based on the gradient descent algorithm. The method is used to search for the value of the extremal (x^\dagger, u^\dagger) satisfying $\nabla \mathcal{L}(x^\dagger, u^\dagger, z(x^\dagger, u^\dagger)) = 0$.

Algorithm 1

- Step 1: Fix the initial guess $u \in \mathcal{U}_{ad}$ for the control, where each element of u is interpreted as a linear combination of the characteristic functions
- Step 2: Solve the state equation in a forward scheme to calculate x
- Step 3: Calculate the objective function $J(x, u)$
- Step 4: Solve the adjoint equation in a backward scheme to calculate z
- Step 5: Solve the gradient equation to get the descent vector u^* supplemented by x and z in Steps 2 and 4. Use the actual values $\{u_i^*\}_{j=0,1,\dots,\lceil T/h_i \rceil}$ in the particular times $\{t_{i,j}\}_{j=0,1,\dots,\lceil T/h_i \rceil}$ to update the values $u_i^*(t) \mapsto \sum_{0 \leq j \leq \lceil T/h_i \rceil} \{u_i^*\}_j \mathbf{1}_{[t_{i,j}, t_{i,j+1})}(t)$, $i = 1, 2$
- Step 6: Update $u \mapsto u - \kappa u^*$ and saturate u as in (14)
- Step 7: Go to Step 2. Combine this loop with an update (reduction) of the step-length κ by using a sort of approximate line search methods. Do this loop unless some termination criteria are met.

OPTIMAL CONTROL RESULT

It is emphasized that the semi-discrete control must be applied well in the real field. In this paper, we highlight the exact daily-valued control measures in mass unit. We explore the mosquito population dynamics regulated by the additional control measures in order to study the effect of the control to mosquito abundance in the field. It is assumed that the control is conducted in $T = 100$ days. The Temephos spraying is conducted once in $h_1 = 5$ days, meanwhile the thermal fogging is conducted once in $h_2 = 10$ days. Using various combinations of the two control measures and the in-moment initial value, we investigate and compare numerical results from the following scenarios.

Scenario-1: This supplements the dynamical system (2) with the initial value as the size of all compartments when they grow at the earliest time without the presence of the control. We use the initial values united as the vector $[8, 8, 6, 6, 5]$.

Scenario-2: The initial value is taken from the size of all compartments when the growth tends to reach the peak of increment. This currently occurs in one-fourth of the total observation time. The condition is considered without the presence of the control. The initial value is given as the vector $[21, 43, 24, 37, 8]$.

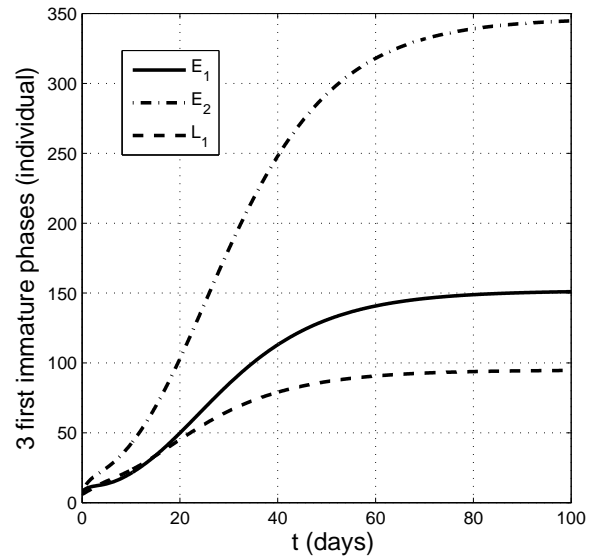


Fig. 3 The uncontrolled trajectory of the indoor egg, the outdoor egg, and the indoor larva.

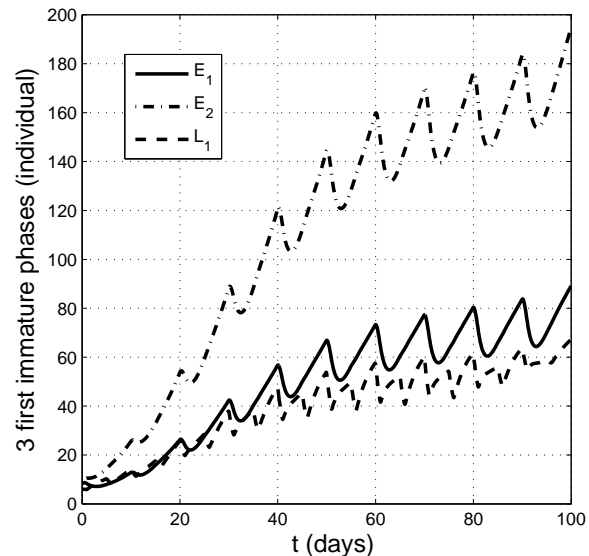


Fig. 4 The controlled trajectory of the indoor egg, the outdoor egg, and the indoor larva.

Scenario-3: The initial value is taken from the size of all compartments when they grow at a half of the total observation time. The condition is considered without the presence of the control. In our preliminary simulation, this time admits the fact that all compartments are at the beginning to reach the positive equilibrium. The initial value is given as the vector $[93, 200, 70, 122, 27]$.

The trade-off coefficients: $\omega_{x,i}, i = 1, \dots, 4$

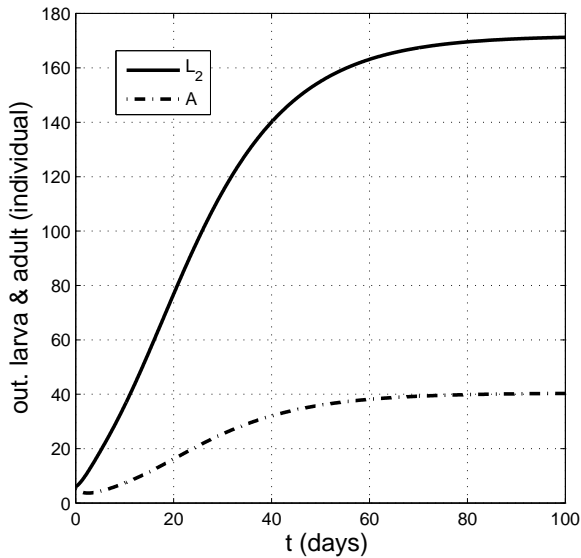


Fig. 5 The uncontrolled trajectory of the outdoor larva and the adult.

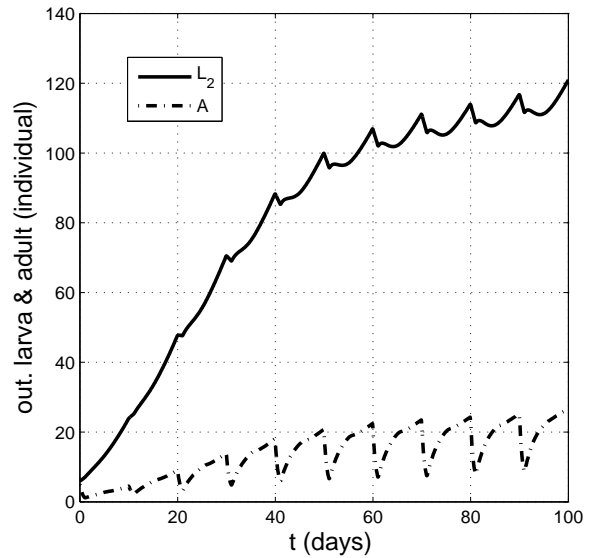


Fig. 6 The controlled trajectory of the outdoor larva and the adult.

and $\omega_{u,i}$, $i = 1, 2$, which are used in the objective function, are given as $\omega_{x,1} = \omega_{x,2} = \omega_{x,3} = \omega_{x,4} = 1$, $\omega_{x,5} = 2$, and $\omega_{u,1} = \omega_{u,2} = 400.000$. The guessed initial value for the control is taken to which satisfy the limitation $0 \leq u_i(t) \leq 1.5$ mg, $i = 1, 2$ for all t in $[0, T]$. We give the value for each parameter as follows: $m = 1.5$, $p = 0.4$, $\phi = 3$ (1/day), $\alpha_1 = 0.3$ (1/day), $\alpha_2 = 0.2$ (1/day), $\alpha_3 = 0.08$ (1/day), $\alpha_4 = 0.05$ (1/day), $q_1 = 0.04$, $q_2 = 0.05$, $q_3 = 0.05$, $w_1 = 1.0$ (1/mg \times 1/day), $w_2 = 1.5$ (1/mg \times 1/day), $\sigma_1 = 0.004$ (1/individual \times 1/day), $\sigma_2 = \sigma_1/m$ (1/individual \times 1/day), $\mu_1 = 0.02$ (1/day), $\mu_2 = 0.01$ (1/day), $\mu_3 = 0.02$ (1/day), $\mu_4 = 0.01$ (1/day), $\mu_5 = 0.4$ (1/day).

The controlled trajectory defines the dynamics of the size of a particular compartment under the optimal control. The uncontrolled trajectory defines the dynamics of the size of a particular compartment without the optimal control. Fig. 3 and Fig. 4 clearly illustrate the uncontrolled trajectory and controlled trajectory of the indoor egg, the outdoor egg, and the indoor larva. It is seen from the figures that all the controlled trajectories are lied in the range below all the associated uncontrolled trajectories. This means that the optimal control makes significant suppression to all dynamics of the size of the first three *A. aegypti* compartments.

In a same viewpoint, Fig. 5 and Fig. 6 illustrate the uncontrolled trajectory and the controlled trajectory of the outdoor larva and the adult. We end up with the same conclusion that the optimal control can

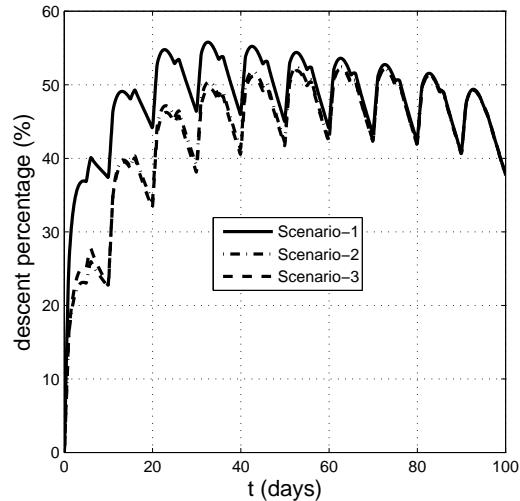


Fig. 7 The descent percentage D .

significantly suppress the size of the outdoor larva and the prospective dengue vector. It is clearly seen from Fig. 6 that all the shock-points illustrated in the controlled trajectory of the adult remain under 10 units during the observation time. This situation seemingly supports human effort in combating the spread of dengue fever.

We define the descent percentage D , where it formulates the percentage of the difference between the sum of all uncontrolled trajectories and the sum of all controlled trajectories over the sum of all uncontrolled trajectories. Fig. 7 shows that D increases with time.

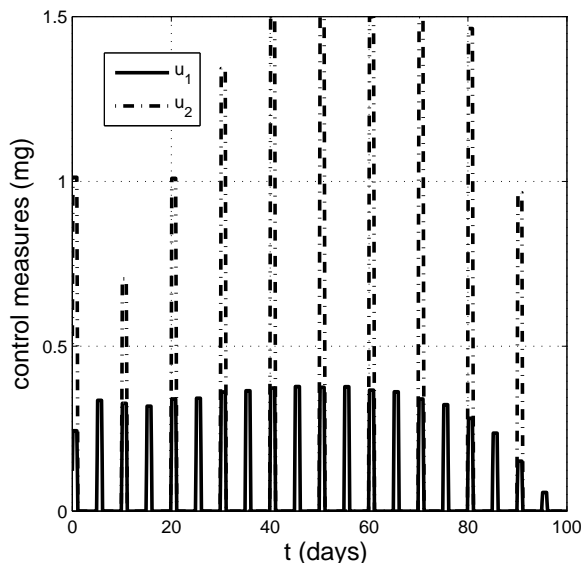


Fig. 8 Trajectories of the optimal control for Scenario-1.

The figure indicates that the most significant decline occurs in Scenario 1. It is also seen from the figure that the first 25 days of observation can be accounted as the days when the control effort needs to be improved in order to produce an optimal estimation of the cost. Resembling with computing D , we find that the total size of all compartment's endpoints when both control measures are at present tends to reach the least value comparing to that when one control measure vanishes.

Fig. 8 shows that the mass profile of the thermal fogging is in greater range than that of the Temephos spraying for Scenario-1. We find the same result for Scenario-2 and Scenario-3. These results, derived from the model, suggest that the thermal fogging plays an important role in suppression of the size of *A. aegypti* population in the field. We find also that the mass profile of the thermal fogging rises from Scenario-1 to Scenario-3. Meanwhile, the mass profile of the Temephos spraying is almost stagnant. A combination of these results with the result described in Fig. 2 shows that the mass of the thermal fogging needs to be enhanced rather than the mass of the Temephos spraying during the observation time.

CONCLUSIONS

An optimal control problem is constructed in this paper based on the mosquito population dynamics regulated by the two control measures: the Temephos spraying and the thermal fogging. In the presence of the constant control, a value combination of the control measures in the domain $[0, 0.4]^2$ still gives a life-coexistence among all compartments in the

model. The basic mosquito offspring is obtained from the maximum of the modulus of all elements in the spectrum of the next generation matrix. This number can be used as an indicator to both analyse the stability of the mosquito-free equilibrium and describe the sensitivity of each control measure. Preliminary simulation result shows that the mosquito-free equilibrium (referred to as the trivial equilibrium) is always unstable for any choice of the constant control measures undertaken in the simulation. A combination of the existence and stability of the positive non-trivial equilibrium state and the instability of the trivial equilibrium, leads us to the early hypothesis, that there is always a life-coexistence among all compartments after applying a constant control in the range undertaken in the simulation. Whereas the constant control seems less applicable in everyday life, an optimal control is required such that the balance between minimizing the cost for the control and suppressing the trajectory of all compartments is achieved together. From our optimal control simulation, the results show that all the controlled trajectories are lied under all the associated uncontrolled trajectories after performing the optimal control. From every specific scenario of the control implementation, we conclude that one needs to enhance the mass of the thermal fogging rather than the mass of the Temephos spraying during the observation time.

Acknowledgements: This study was financially supported by HIBAH PRI ITB 2011.

REFERENCES

1. Vasconcelos PFC, Travassos Da Rosa APA, Coelho ICB, Menezes DB, Travassos Da Rosa ES, Rodrigues SG, Travassos Da Rosa JFS (1998) Involvement of the central nervous system in dengue fever: three serologically confirmed cases from Fortaleza, Ceará, Brazil. *Rev Inst Med Trop S Paulo* **40**, 35–40.
2. Gubler DJ (1998) Dengue and dengue hemorrhagic fever. *Clin Microbiol Rev* **11**, 480–96.
3. Otero M, Schweigmann N, Solari H (2008) A stochastic spatial dynamical model for *Aedes aegypti*. *Bull Math Biol* **70**, 1297–325.
4. Almeida JS, Ferreira RPM, Eiras AE, Obermayr RP, Geier M (2010) Multi-agent modeling and simulation of an *Aedes aegypti* mosquito population. *Environ Model Software* **25**, 1490–507.
5. Ko CY, Koon LL, Yin PF (2001) Detection of dengue viruses in field caught male *Aedes aegypti* and *Aedes albopictus* (Diptera: Culicidae) in Singapore by type-specific PCR. *J Med Entomol* **38**, 475–9.
6. Thomas SJ, Endy TP (2011) Vaccines for the prevention of dengue: Development update. *Landes Bio-science Inc* **7**, 674–84.

7. Huy NT, Giang TV, Thuy DHD, Kikuchi M, Hien TT, Zamora J, Hirayama K (2013) Factors associated with dengue shock syndrome: A systematic review and meta-analysis. *PLoS Negl Trop Dis* **7**, e2412.
8. Lek-Uthai U, Ratthanaprechachai P, Chowanadisai L (2011) Bioassay and effective concentration of Temephos against *Aedes aegypti* larvae and the adverse effect upon indigenous predators: *Toxorychites splendens* and *Micronecta* sp. *Asia J Publ Health* **2**, 67–77.
9. Nazni WA, Lee HL, Rozita WMW, Lian AC, Chen CD, Azahari AH, Sadiyah I (2009) Oviposition behaviour of *Aedes albopictus* in Temephos and *Bacillus turingiensis*-treated ovitraps. *Dengue Bull* **33**, 209–17.
10. Clemons A, Haugen M, Flannery E, Tomchaney M, Kast K, Jacowski C, Le C, Mori A, Holland WS, Sarro J, Severson DW, Duman-Scheel M (2010) *Aedes aegypti*: An emerging model for vector mosquito development. Cold Spring Harb Protoc 2010.
11. Lea AO, Briegel H, Lea HM (1978) Arrest, resorption, or maturation of oocytes in *Aedes aegypti* dependence on the quantity of blood and the interval between meals. *Physiol Entomol* **3**, 309–16.
12. Gomes Ad-C, Gotlieb SLD, Marques CCd-A, de Paula MB, Marques GRAM (1995) Duration of larval and pupal development stages of *Aedes albopictus* in natural and artificial containers. *Rev Saúde Pública* **29**, 15–9.
13. Peters TM, Chevone BI, Greenough NC, Callahan RA, Barbosa P (1969) Intraspecific competition in *Aedes aegypti* (L.) larvae. I. Equipment, techniques, and methodology. *J Am Mosq Contr Assoc* **29**, 667–74.
14. Trpis M, Hausermann W (1986) Dispersal and other population parameters of *Aedes aegypti* in an African village and their possible significance in epidemiology of vector-borne diseases. *Am J Trop Med Hyg* **35**, 1263–79.
15. Caetano MAL, Yoneyama T (2001) Optimal and sub-optimal control in dengue epidemics. *Optim Contr Appl Meth* **22**, 63–73.
16. Thomé RCA, Yang HM, Esteva L (2010) Optimal control of *Aedes aegypti* mosquitoes by the sterile insect technique and insecticide. *Math Biosci* **223**, 12–23.
17. Driessche VD, Watmough J (2002) Reproduction numbers and sub-threshold endemic equilibria for compartmental models of disease transmission. *Math Biosci* **180**, 29–4.
18. Hocking LM (1991) *Optimal Control: An Introduction to the Theory and Application*, Oxford Univ Press, New York.